

A Search for Di-lepton Signatures from Minimal Low Energy Supergravity in $\bar{p}p$ Collisions at $\sqrt{s} = 1.8$ TeV

The D \emptyset Collaboration ^{*}

Fermi National Accelerator Laboratory, Batavia, Illinois 60510

(May 19, 2019)

Abstract

We report on a search for supersymmetry using the D \emptyset detector. The 1994-96 data sample of $\sqrt{s} = 1.8$ TeV $\bar{p}p$ collisions was analyzed for events containing two leptons (e or μ), two or more jets, and missing transverse energy. Assuming minimal supergravity, with free parameters m_0 , $m_{1/2}$ and $\tan\beta$, various thresholds were employed to optimize the search. No excess of events was observed. We present exclusion contours in the $(m_0, m_{1/2})$ plane for $\tan\beta = 2 - 6$.

^{*}Submitted to the *International Europhysics Conference on High Energy Physics, EPS-HEP99*, 15 – 21 July, 1999, Tampere, Finland.

Supersymmetric extensions of the Standard Model (SM) have been the subject of intense theoretical and experimental investigation in recent years. The simplest extension, the Minimal Supersymmetric Standard Model (MSSM), incorporates supersymmetry (SUSY) [1], a fundamental space-time symmetry relating fermions and bosons, by requiring a supersymmetric partner (sparticle) for every SM particle, and an additional Higgs doublet. The added assumption of conservation of R -parity, a multiplicative quantum number (+1 for SM particles and -1 for their SUSY counterparts), implies pair production of sparticles in high energy collisions and subsequent sparticle decay either directly or via lighter sparticles into a final state containing SM particles and two stable, lightest supersymmetric particles (LSP). The LSP [2], which is weakly interacting, escapes detection leading to a large apparent imbalance in transverse momentum (\cancel{E}_T) in the event — a characteristic signature for SUSY.

Because of the large number free parameters in the generic MSSM, we have chosen to compare our data with a class of Minimal Low Energy Supergravity (mSUGRA) models [3] that are more tightly constrained. These are parametrized in terms of only five free parameters: a common SUSY-breaking scalar mass (m_0) for all scalars, a common mass for all gauginos ($m_{1/2}$), a common value for all trilinear couplings (A_0), the ratio of the vacuum expectation values of the two Higgs fields ($\tan\beta$) and the sign of μ , where μ is the Higgsino mass mixing parameter.

In this letter we describe a search for associated production of squarks (\tilde{q}), gluinos (\tilde{g}), charginos ($\tilde{\chi}_{1-2}^\pm$), and/or neutralinos ($\tilde{\chi}_{1-4}^0$), and consider final states containing two isolated leptons (e or μ), jets, and \cancel{E}_T [4]. Cascade decays of these particles can have significant leptonic branching fraction. Therefore, leptonic SUSY searches complement searches that consider only jets and \cancel{E}_T [5].

The DØ detector [6] consists of a hermetic cylindrical liquid argon calorimeter surrounding central tracking chambers and enclosed by an iron toroidal muon spectrometer. The calorimeter is divided into pseudorapidity (η) regions: central (CC), $0 \leq |\eta| \leq 1.2$, and two end caps (EC) $1.5 \leq |\eta| \leq 2.5$. Pseudo-projective towers radiate from the interaction point with segmentation of 0.1×0.1 in η - ϕ space. The third electromagnetic (EM) layer (EM3) has finer segmentation (0.05×0.05). Within the central tracking chambers, a transition radiation detector (TRD) aids in electron identification in the CC. The muon system is demarcated into two η ranges. Chambers parallel to the beam subtend $0 \leq |\eta| \leq 1.0$, and chambers perpendicular to the beam subtend $1.0 \leq |\eta| \leq 2.5$. There are three main layers of muon chambers, one before and two after the magnetic field.

The data was collected in the 1994-96 Tevatron collider run. We triggered on an electron, one jet, and \cancel{E}_T for ee and $e\mu$ signatures, and on a single muon and jet for the $\mu\mu$ signatures. The analyzed luminosity was 108 pb^{-1} for ee and $e\mu$ signatures, and 103 pb^{-1} for $\mu\mu$ signatures. The original data sample, approximately 40 million events, was reduced by requiring that the e +jet or μ +jet triggers have two leptons satisfying loose identification criteria, two jets with $E_T > 15 \text{ GeV}$, and $\cancel{E}_T > 14 \text{ GeV}$. This sample of 24,233 events (1,395 ee , 8,063 $e\mu$, and 18,674 $\mu\mu$) was used in the subsequent offline analysis.

Jets were reconstructed as cones of radius $R = \sqrt{(\Delta\eta)^2 + (\Delta\phi)^2} = 0.5$. Jet quality cuts, designed to remove instrumental and cosmic ray background, rejected events with extreme values of energy concentrated in the EM layer, the outer coarse hadronic layer, or in any

single cell. The loss in efficiency from rejecting these backgrounds, which scaled linearly with jet E_T , was about 1% at 20 GeV and 1.5% at 200 GeV [7]. The jet energy scale was determined from γ +jet events, by balancing the E_T of the jet against that of the photon [8].

Electrons were reconstructed by clustering energies deposited in towers of the calorimeter, and requiring the fraction of energy in the EM layers (EM fraction) to be at least 90%. The EM energy scale was determined from di-electron events using the known Z boson, J/ψ , and π^0 mass values [9].

We selected CC electrons using a 5-variable (4-variable for the EC) Neyman-Pearson likelihood function based on EM fraction, a shower-shape variable, dE/dx in the central detector, the quality of the match between the reconstructed track and the cluster center of gravity in the EM3 layer (σ_{TRK}), and ϵ_{TRD} , a variable based on the energy deposited in the TRD (ϵ_{TRD} was not used for the EC). The identification efficiency for electrons was determined from a sample of $Z \rightarrow ee$ events, and is a function of the jet multiplicity (high track multiplicity degrades the resolution and efficiency of σ_{TRK}). We defined the electron isolation $I = (E_{\text{tot}}^{0.4} - E_{\text{EM}}^{0.2})/(E_{\text{EM}}^{0.2})$, where $E_{\text{EM}}^{0.2}$ is the EM energy in a cone of $R = 0.2$, and $E_{\text{tot}}^{0.4}$ is the total energy in a cone of $R = 0.4$. We required $I < 0.3$ in this analysis. The identification efficiencies for isolated electrons were typically (78-84)% for CC electrons, and (63-69)% for EC electrons.

Muon identification is detailed in Ref. [10]. Muons were identified by detecting tracks in the muon chambers. A global fit combined these tracks with tracks in the central detector and ionization energy in the calorimeter. Muons were required to be isolated: they had to lie outside of all reconstructed jets with cones $R = 0.5$. To remove poorly measured muons, the direction of the vector \cancel{E}_T was required to be more than 10 degrees away from any muon track (this reduced muon acceptance by about 10% per muon).

There was a 75% chance of a second interaction occurring during a recorded hard-scattering event. To avoid large apparent \cancel{E}_T from misidentified vertices caused by such extra interactions, we defined the hard interaction vertex by the nominal beam center and the average longitudinal position of the two leptons (except for $e\mu$ events, where the position of the electron provided better resolution). The vertex was also required to be within ± 60 cm of the center of the detector. This requirement was $(98.1 \pm 0.8)\%$ efficient [4], guaranteed good fiducial acceptance, and removed events with erroneous vertex assignments.

Our data sample was further reduced by requiring two good jets with $E_T > 20$ (all thresholds are in GeV), $\cancel{E}_T > 20$, and offline leptons as follows: $E_T(e_1) > 17$ and $E_T(e_2) > 15$, or $E_T(e) > 17$ and $E_T(\mu) > 4$, or $E_T(\mu_1) > 20$ and $E_T(\mu_2) > 10$. This final sample contained 10 ee , 6 $e\mu$, and 3 $\mu\mu$ events.

Background was comprised of four sources: top, Z , W , and QCD jet production. The top and Z backgrounds were calculated using measured cross sections and a fast detector-simulation package (described below). QCD multijet and W + jet backgrounds were estimated from data samples. For ee and $e\mu$ signatures, we selected events that would have been candidates, except for missing one isolated electron, but having instead an extra jet. The background was estimated using the measured probability of one of the jets being misidentified as the missing isolated electron [4]. For $\mu\mu$ signatures, the background sample had one isolated and one non-isolated muon, and an extra jet. The measured probability of a non-isolated muon to appear as an isolated muon was used to estimate the background from this source [10]. The QCD/ W + jet backgrounds were combined because they cannot

be separated: for W boson events the identified lepton is real, and for QCD the identified lepton is due to a fluctuation.

The usual way to search for signal is to generate signal and background events, and to optimize a single set of requirements that yield best discrimination. The problem with this method is that the optimum thresholds vary as a function of the mSUGRA input parameters. In essence, one must tune requirements at every point in model space, which is exceptionally demanding in computing resources.

We performed an approximate optimization of selection criteria on a grid of thresholds. For ee signatures, we considered sets of requirements both with and without any extra selection on the ee invariant mass (M_{ee}), used to reduce background from Z bosons. For $\mu\mu$ signatures, a cut of $\cancel{E}_T > 40$ GeV provided the lowest Z boson background. Each unique combination of thresholds is called a *channel*. In all, we defined 52 channels (16 ee , 24 $e\mu$, and 12 $\mu\mu$), most of which are enumerated in Table I.

To handle the large number of channels, a specialized fast Monte Carlo was written [4] that incorporated SPYTHIA [11] as event generator, simulation of detector, trigger, and particle identification tuned to data, and a package that kept track of the probability for produced events to be observed in any of the 52 channels. The primary output were efficiencies $\epsilon_i = BR \cdot e_{\text{TRIG}} \cdot e_{\text{ID}} \cdot a_{\text{DET}}$ (products of the branching fraction, trigger efficiency, identification efficiency, and detector acceptance, respectively) for each channel i , and the production cross section.

Because looser requirements produced event samples that were supersets of tighter requirements, the channels within a given signature were necessarily correlated. To avoid bias, we chose a “best” channel for each signature (for each set of mSUGRA parameters), based on the background estimate and expected signal. Specifically, for each channel, we defined an expected significance, $\bar{S}_i = \sum_{N=0}^{\infty} P(s_i + b_i | N) \cdot S(b | N)$ [12], where P is the (Poisson) probability that signal (s_i) and background (b_i) produce N observed events, and S is the (Gaussian) significance, that is, the number of standard deviations that background must fluctuate to produce N events. For each set of mSUGRA parameters (model) k , we thus obtained three independent, optimized search channels: ee_{best}^k , $e\mu_{\text{best}}^k$, and $\mu\mu_{\text{best}}^k$. The single best two-channel or three-channel combination was also determined (cmb_{best}^k), with best again defined in terms of expected significance. For each model k , we calculated four 95% confidence limits on the cross section, using the determined best channels and a standard Bayesian prescription, with a flat prior for the cross section for signal [13].

We also calculated a model-independent limit for the product $\epsilon \cdot \sigma$. Table I summarizes the background prediction and number of observed events in each channel. Also shown is the (one-sided Poisson) probability that the background fluctuated to produce the events observed.

We generated about 10,000 points (20,000 events each) randomly distributed in the space $0 < m_0 < 300$ GeV/c², $10 < m_{1/2} < 110$ GeV/c², and $1.2 < \tan \beta < 10$, to obtain a rough exclusion contour. We use this contour to select specific ranges in m_0 and $m_{1/2}$ around which to generate higher statistics samples (150,000 - 200,000 events each) for fixed $\tan \beta$. Figure 1 shows the 95% exclusion contours for various $\tan \beta$ values. For $\tan \beta$ greater than 6.0, we do not exclude any models that were not previously excluded by LEP I [14].

Clearly, the contours in Fig. 1 have structure. First, the dip near $m_0 = 80$ GeV/c² is caused by the dominance of the decay $\tilde{\chi}_2^0 \rightarrow \nu\bar{\nu}\tilde{\chi}_1^0$ over charged leptons for this part of phase

Signature: $ee + jets + \cancel{E}_T$							
j_1	N_{jets}	\cancel{E}_T	Background	Data	Prob. (%)	$(\epsilon\sigma)_{\text{lim}} \text{ (fb)}$	
20	2	20	10.67 ± 1.24	10	50.1	85	
20	3	20	3.08 ± 0.39	2	40.3	42	
20	2	30	4.72 ± 0.65	2	15.0	43	
20	3	30	1.28 ± 0.21	1	63.4	42	
45	2	20	7.56 ± 0.94	5	23.5	58	
45	3	20	2.49 ± 0.33	0	8.3	31	
45	2	30	3.26 ± 0.51	2	36.7	45	
45	3	30	1.18 ± 0.20	0	30.7	31	
Signature: $ee + jets + \cancel{E}_T$, exclude $80 < M_{ee} < 105$							
20	2	20	4.84 ± 0.69	5	52.5	67	
20	3	20	1.27 ± 0.21	1	63.8	40	
20	2	30	4.02 ± 0.58	1	9.0	37	
20	3	30	0.86 ± 0.17	1	57.2	44	
45	2	20	3.03 ± 0.48	3	64.0	60	
45	3	20	0.93 ± 0.17	0	39.5	31	
45	2	30	2.16 ± 0.41	2	63.2	53	
45	3	30	0.80 ± 0.16	0	44.9	31	
Signature: $\mu\mu + jets + \cancel{E}_T$							
20	2	20	1.61 ± 0.26	3	22.1	68	
20	3	20	0.37 ± 0.10	2	5.6	66	
20	2	30	0.75 ± 0.19	2	17.6	60	
20	3	30	0.16 ± 0.07	1	14.7	49	
20	2	40	0.53 ± 0.16	1	40.4	46	
20	3	40	0.13 ± 0.06	1	12.2	49	
45	2	20	1.28 ± 0.24	3	14.2	71	
45	3	20	0.34 ± 0.09	2	4.8	65	
45	2	30	0.65 ± 0.18	2	14.2	61	
45	3	30	0.16 ± 0.07	1	14.7	49	
45	2	40	0.45 ± 0.15	1	35.5	47	
45	3	40	0.12 ± 0.06	1	11.4	50	
Signature: $e\mu + jets + \cancel{E}_T$							
μ	j_1	N_{jets}	\cancel{E}_T	Background	Data	Prob. (%)	$(\epsilon\sigma)_{\text{lim}} \text{ (fb)}$
4	20	2	20	6.30 ± 1.04	6	55.9	73
4	20	3	20	1.75 ± 0.31	1	47.6	41
4	45	2	30	1.97 ± 0.47	2	57.2	52
4	45	3	30	0.70 ± 0.16	0	49.7	31
10	20	2	20	2.50 ± 0.57	2	54.4	50
10	20	3	20	0.68 ± 0.17	1	48.6	45
10	20	2	30	1.67 ± 0.49	0	18.8	31
10	20	3	30	0.56 ± 0.15	0	57.2	31
10	45	2	20	1.79 ± 0.49	2	52.0	53
10	45	3	20	0.46 ± 0.14	1	36.3	47
10	45	2	30	1.35 ± 0.44	0	25.9	31
10	45	3	30	0.41 ± 0.13	0	66.4	31

TABLE I. Sample of results for all signatures. For ee , $E_T(e_1) > 17$ GeV and $E_T(e_2) > 15$ GeV. For $\mu\mu$, the requirements were 10 and 20 GeV. For $e\mu$ signatures, each channel required the electron $E_T > 17$ GeV, and the muon E_T as specified (μ). For all signatures, the leading jet E_T is j_1 , and we require N_{jets} with $E_T > 20$ GeV. The error on the background is the sum in quadrature of systematic and statistical errors. The probability is shown that the background fluctuated to produce the number of observed events. $(\epsilon\sigma)_{\text{lim}}$ is the 95% CL exclusion on the product of the total cross section, branching ratio, and all relevant efficiencies.

space. Sensitivity improves for $\tan\beta$ closer to 3.0 due to several factors: gaugino couplings increase, causing the $\tilde{\chi}_2^0$ to preferentially decay into quarks and become a source of jets;

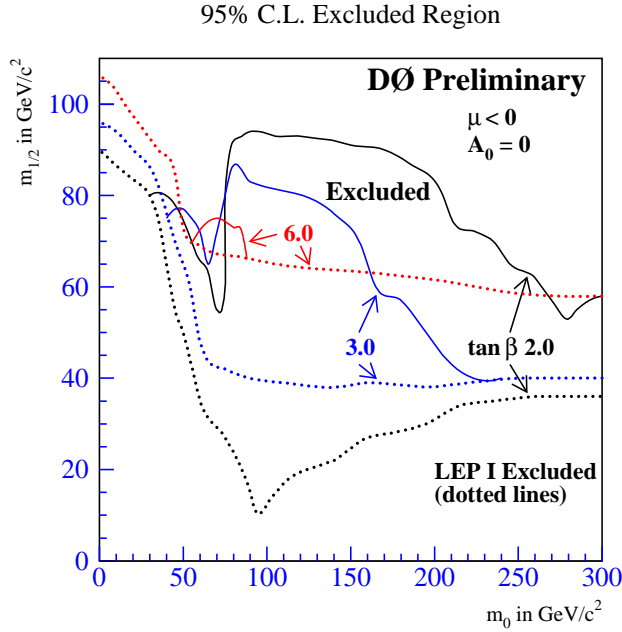


FIG. 1. Exclusion regions at 95% confidence for various $\tan \beta$ values obtained in the di-lepton search.

gaugino masses decrease, and decays of squarks into $\tilde{\chi}_3^0$ and $\tilde{\chi}_4^0$ become allowed; $\tilde{\chi}_3^0$ and $\tilde{\chi}_4^0$ dominantly decay into sneutrinos, $\tilde{\nu}_l$; $\tilde{\nu}_l \rightarrow \tilde{\chi}_1^\pm l^\mp$ dominates in this region, and becomes a source of leptons. Sensitivity decreases again for $\tan \beta$ values around 7.0, where decays into light charged leptons are reduced by increased couplings to large mass fermions. Second, the exclusion for $m_{1/2}$ falls as m_0 increases, corresponding to the region where $m_{\tilde{q}} \gg m_{\tilde{g}}$, and the contribution of squark production is thereby lost. Overall, our data exclude gluinos below 129 GeV/c^2 and squarks below 138 GeV/c^2 , for $m_0 < 300 \text{ GeV}/c^2$ and $\tan \beta < 10.0$.

In conclusion, we have presented a search for di-lepton signatures from squark, gluino, and gaugino production. No significant excess was observed and limits and exclusion contours were presented as a function of mass parameters in the mSUGRA model.

We thank Chris Kolda, Steve Mrenna, Greg Anderson, Jim Wells, and Gordon Kane for helpful discussions. We thank staffs at Fermilab and collaborating institutions for contributions to this work, and acknowledge support from the Department of Energy and National Science Foundation (USA), Commissariat à L'Energie Atomique (France), Ministry for Science and Technology and Ministry for Atomic Energy (Russia), CAPES and CNPq (Brazil), Departments of Atomic Energy and Science and Education (India), Colciencias (Colombia), CONACyT (Mexico), Ministry of Education and KOSEF (Korea), and CONICET and UBACyT (Argentina).

REFERENCES

- [1] X. Tata, in *The Standard Model and Beyond*, edited by J. Kim (World Scientific, Singapore, 1991); H. Nilles, Phys. Rep. **110**, 1 (1984); P. Nath *et al.*, *Applied $N = 1$ Supergravity*, ICTP Series in Theoretical Physics Vol. 1 (World Scientific, Singapore, 1984); H. Haber and G. Kane, Phys. Rep. **117**, 75 (1985).
- [2] For the model under consideration $\tilde{\chi}_1^0$, the lightest neutralino, is the LSP over most of the SUGRA parameter space.
- [3] G. L. Kane *et al.*, Phys. Rev. D **49**, 6173 (1994); H. Baer and X. Tata, Phys. Rev. D **47**, 2739 (1993); M. Drees and M. M. Nojiri, Nucl. Phys. **B 369**, 54 (1992); L. E. Ibanez, C. Lopez and C. Munoz, Nucl. Phys. **B 256**, 218 (1985).
- [4] R. J. Genik II, Ph.D. Thesis, Michigan State University (unpublished). http://www-d0.fnal.gov/results/publications_talks/thesis/thesis.html
- [5] B. Abbott, *et al.*, Submitted to Phys. Rev. Lett., hep-ex/9902013.
- [6] B. Abbott, *et al.*, Nucl. Instr. and Methods, **A338**, 185 (1994).
- [7] L. Babukhadia, *et al.*, DØ Note 3407 (unpublished).
- [8] B. Abbott, *et al.*, Nucl. Instr. and Methods, **A424**, 352 (1999). hep-ex/9805009.
- [9] B. Abbott, *et al.*, Submitted to Phys. Rev. **D**, [58] 092003 (1998).
- [10] B. Abbott, *et al.*, hep-ex/9808029. Submitted to Phys. Rev. D.
- [11] SPYTHIA is a superset of PYTHIA 5.7 [15], allowing us to generate Standard Model backgrounds. We incorporate routines developed by Kolda [16] to generate the mSUGRA model spectrum. This spectrum is passed to SPYTHIA using the general MSSM option. S. Mrenna, ANL-HEP-PR-96-63 (unpublished).
- [12] J. Linnemann, at Computing in High Energy Physics, Rio De Janeiro, September 1995. World Scientific (1996), pp. 205-209.
- [13] I. Bertram *et al.*, DØ Note 3476 (unpublished); also see Particle Data Group, R. M. Barnett *et al.*, Phys. Rev. D **54**, 165 (1996).
- [14] The combined results of Z pole collisions from ALEPH, DELPHI, L3, and OPAL collaborations. Particle Data Group, R. M. Barnett *et al.*, Phys. Rev. **D**, **54**, 165 (1996).
- [15] T. Sjöstrand, CERN-TH.7112/93, (1993).
- [16] G. L. Kane, C. Kolda, L. Roszkowski, and J. Wells, Phys. Rev. **D**, **49** 6173-6219 (1994).